View metadata, citation and similar papers at core.ac.uk
brought to you by CORE
provided by Repository@USM

DESIGN AND DEVELOPMENT OF AN INDOOR REAL-TIME LOCATING SYSTEM

by

MOHAMED MOHAMED MOHAMED ELHEFNAWY

Thesis submitted in fulfillment of the requirements
for the degree of
Doctor of philosophy

January 2010

SCHOOL OF ELECTRICAL AND ELECTRONIC ENGINEERING
UNIVERSITI SAINS MALAYSIA

REKA BENTUK DAN PEMBANGUNAN SUATU SISTEM LOKASI MASA-SEBENAR DALAMAN

ABSTRAK

Beberapa teknologi lokasi telah dibangunkan dan secara komersialnya telah digunakan secara berkesan termasuklah Sistem Kedudukan Sejagat (Global Positioning System, GPS) dan sistem khidmat 911 tertingkat wayarles (E-911). Namun demikian, teknologi ini digunakan khusus untuk aplikasi luar dan tidak begitu berkesan jika digunakan di dalam bangunan atau di kawasan Bandar yang padat. Kebanyakan sistem lokasi dalaman komersial yang ada agak lemah prestasinya kerana wujudnya hinggar, gangguan, hilang laluan, pengutuban yang tidak sepadan, pantulan pengutuban dan kesan fenomena pelbagai laluan dalam saluran wayarles. Oleh itu, suatu sistem lokasi yang mempunyai prestasi yang baik untuk persekitaran yang tertutup amat diperlukan. Di dalam disertasi ini, pelbagai aspek teknikal yang meluas serta isu-isu yang mencabar, yang terlibat dalam pembangunan sistem lokasi dalamam dibincangkan. Yang pertama dibincangkan adalah reka bentuk dan pelaksanaan sistem antena RTLS, diikuti dengan memperkenalkan suatu teknik baru untuk menganggar sudut tiba (angle-of-arrival, AOA). Yang terakhir, dibincangkan tentang pembangunan dan pelaksanaan matematik bagi penganggar masa tiba (time-of-arrival, TOA). Dapatan menunjukkan bahawa, penggunaan hibrid kuadratur sebagai penyuap bagi antena mikrojalur tampal segi empat sama (square patch microstrip antenna) melalui dua bukaan yang menghasilkan kepelbagaian pengutuban bulat (circular polarization diversity), lebar-jalur yang lebar dan nisbah paksi yang baik, di samping meminimumkan saiz antena. Matriks 4×4

Butler juga dilaksanakan sebagai rangkaian penyuap (feeding network) bagi susunan antena mikrojalur 2×2 yang menjana empat alur yang mempunyai kepelbagaian pengutuban bulat, gandaan yang tinggi, nisbah paksi yang baik dan lebar-jalur yang lebar. Dapatan disertasi ini juga menunjukkan bahawa teknik yang dicadangkan untuk menganggar AOA secara signifikannya mampu meningkatkan resolusi tanpa memerlukan nisbah isyarat-hinggar (signal to noise ratio, SNR) yang tinggi. Tambahan pula, AOA boleh dianggar tanpa menggunakan pensampelan ruang, maka keperluan perkakasan / hadwer adalah lebih kecil dibandingkan dengan kaedah yang lain. Dalam penganggaran TOA dengan menggunakan algoritma pengelasan isyarat pelbagai, suatu teknik baru telah dibangunkan bagi menganggar bilangan laluan isyarat yang diterima dan juga untuk menentukan pseudospektrum MUSIC. Prestasi penganggar TOA dipertingkatkan melalui pengurangan kesan rebakan dan pemudaran tertunda pelbagai laluan melalui penggunaan teknik penebalan sifat (zero-padding) dan teknik Matriks Korelasi Ke Depan (Forward Correlation Matrix, FCM). Pertambahan kadar pensampelan akan meningkatkan resolusi penganggar TOA. Sementara itu, julat yang maksimum dapat ditingkatkan apabila bilangan sampel per rangka turut meningkat. Penggunaan saringan Kalman dapat meningkatkan ketepatan dan kejituan penganggar TOA yang dicadangkan. Sistem antena RTLS telah direka bentuk dan dirangsang pada frekuensi resonan 2.437 GHz menggunakan sistem reka bentuk maju dan perisian Matlab. Pengukuran corak pancaran dan nisbah paksi dijalankan berdekatan dengan kebuk medan Satimo. Teknik pemprosesan isyarat yang dibangunkan untuk RTLS dirangsang menggunakan perisian Simulink. Keberkesanan teknik pemprosesan isyarat ini terbukti melalui pelaksanaan perkakasan masa sebenar pada bod platform pembangunan SDR (software-defined radio) SFF (small form factor).

DESIGN AND DEVELOPMENT OF AN INDOOR REAL-TIME LOCATING SYSTEM

ABSTRACT

Several locating technologies have been developed and commercially deployed including the Global Positioning System (GPS) and the wireless enhanced 911 service system (E-911), but these locating technologies are used mainly for outdoor location-based applications and can not be used effectively inside buildings and in dense urban areas. Most of the commercial indoor localization systems provide a poor performance due to the presence of noise, interference, path loss, polarization mismatch, polarization reflection and the effect of the multi-path phenomenon in the wireless channel. Therefore, there is a need for a locating system which has a good performance in indoor environments . In this thesis, a wide variety of technical aspects and challenging issues involved in the development of indoor locating systems are discussed. The design and implementation of Real Time Locating Systems (RTLS) antenna system are presented first, then a new technique to estimate the Angle-Of-Arrival (AOA) is introduced, finally model development and implementation for the Time-Of-Arrival (TOA) estimator are discussed.

It is shown that, the use of a quadrature hybrid as a feeder to the square patch microstrip antenna through two apertures produces circular polarization diversity, wide bandwidth and good axial ratio, besides minimizing the antenna size. Also the implementation of the 4×4 Butler matrix as a feeding network to the 2×2 microstrip antenna array generates four beams that have circular polarization diversity, high gain, good axial ratio and wide

bandwidth. In this thesis, the proposed technique to estimate the AOA improves the accuracy significantly without requiring high Signal to Noise Ratio (SNR). Moreover, as the AOA can be estimated without spatial sampling, the hardware requirements are less compared to the other methods.

For the TOA estimation using MUltiple SIgnal Classification (MUSIC) algorithm, new techniques have been developed to estimate the number of paths of the received signal and to find the MUSIC pseudo-spectrum. The performance of the TOA estimator is enhanced by reducing the effects of multipath delay spread and fading by using zero-padding and Forward Correlation Matrix (FCM) techniques. Increasing the sampling rate enhances the resolution of the TOA estimator, while the maximum range can be increased as the number of the samples per frame is increased. The use of Kalman filtering enhances the accuracy and the precision of the proposed TOA estimator.

The RTLS antenna system has been designed and simulated at a resonant frequency equal to 2.437 GHz using advanced design system and Matlab software. Radiation pattern and axial ratio measurements have been carried out in a near field Satimo chamber. The developed signal processing techniques for RTLS have been simulated using Simulink software. The effectiveness of this signal processing techniques has been proved using real time hardware implementation of the Small Form Factor (SFF) Software-Defined Radio (SDR) Development Platform board.

ACKNOWLEDGMENTS

I would like to express my sincere gratitude to my supervisor Dr. Widad Ismail for her invaluable guidance and suggestions and providing all the required facilities for this research. Her inspiration, encouragement and constructive comments were the motive forces behind the successful completion of my work. I am also deeply grateful to my co-supervisor Dr. Shahrel Azmin Suandi for his valuable support and advice throughout this study. In the communication Laboratory, I was always assisted by the staff who were very friendly and cooperative; my special thanks go to Mr. Abdul Latip Abdul Hamid, Mr. Mohamadariff Othman and Wan Nur Hafsha Bt Wan Kairuddin.

I would also like to thank all my friends in our campus for their cooperation and company. Special mention should be made for Mutamed Alkhatib and Sami Salama. A special thanks is given to Mr. Por Chee Seong from Amphenol Malaysia Sdn Bhd company who helped tremendously for some of the measurements in this work. Words can not express my gratefulness to my dear family, especially to my parents for having faith in me and their generosity in love.

To my loving wife Doaa, I give my love and gratitude. As I worked on this research you have endured many sacrifices without any complaints and you have always been there to encourage and support me. To my sons Ali and Omar; thanks for forgiving me for the hours spent away from you and for your unconditional love. Finally, I express my gratitude to the wonderful Malaysian people who gave their kindly help to me during my stay in Malaysia.

TABLE OF CONTENTS

ABSTRAK ii
ABSTRACT iv
ACKNOWLEDGMENTS vi
TABLE OF CONTENTS vii
LIST OF TABLES x
LIST OF FIGURES xi
LIST OF ABBREVIATIONS xv
LIST OF SYMBOLS xvii
CHAPTER 1
INTRODUCTION 1
1.1 Motivation 1
1.2 Problem Statement 2
1.3 Objectives 4
1.3.1 To Combat the Major Impairments of Indoor Wireless Dynamic Environments 4
1.3.2 To Improve the Performance of the Locating System in Indoor Wireless Dynamic Environments 5
1.3.3 Possibility to Minimize Infrastructure and Reduce Hardware Complexity of the Locating System 5
1.4 Contributions of the Thesis 6
1.5 Outline of the thesis. 7
CHAPTER 2
LITERATURE REVIEW 10
2.1 Survey of the Wireless-Based Indoor Positioning Systems 10
2.1.1 GPS 10
2.1.2 WLAN 12
2.1.3 ZigBee 15
2.1.4 UWB 17
2.1.5 Active RFID 19
2.1.6 RTLS 20
2.2 Design and Implementation of Antennas for Indoor Wireless Systems 23
2.2.1 Most Common Methods Employed to Build up Microstrip Antenna 23
2.2.1.1 Feeding Techniques 24
2.2.1.1.1 Microstrip Line Feed 24
2.2.1.1.2 Coaxial Feed 25
2.2.1.1.3 Aperture Coupled Feed 25
2.2.1.1.4 Proximity Coupled Feed 26
2.2.1.2 Methods for the Analysis of Microstrip Antennas 27
2.2.1.2.1 TLM 27
2.2.1.2.2 Cavity Model 28
2.2.1.2.3 Method of Moments (MoM) 28
2.2.2 Previous Works Pertaining to the Design and Implementation of Antennas for Indoor Wireless Systems 29
2.3 Signal Processing Techniques for RTLS 32

2.3.1 Finding the Distance between the Tag and the Reader Based on TOA Value 33
2.3.1.1 Eigen Structure Method 33
2.3.1.2 Maximum Likelihood Method (MLM) 34
2.3.1.3 Direct Sequence Spread Spectrum (DSSS) Method 35
2.3.1.4 Inverse Fourier Transform Method 35
2.3.1.5 Narrowband Signals and Phase Measurement for TOA Estimation 36
2.3.2 Finding the Distance between the Tag and the Reader Based on RSS Value 36
2.3.3 AOA Estimation Methods 37
2.3.3.1 Spectral Estimation Method 37
2.3.3.2 Eigen Structure Method 39
2.3.3.3 Maximum Likelihood Method (MLM) 39
2.3.4 Positioning Methods 40
2.3.4.1 Distance –Based (Tri-lateration) Technique 40
2.3.4.2 Angle-Based (Tri-angulation) Technique 42
2.3.4.3 Hyperbolic Positioning Technique 43
2.3.4.4 Positioning Based on distance/AOA Hybrid 44
2.3.5 Kalman Filtering 45
2.4 Conclusions 46
CHAPTER 3
DESIGN AND IMPLEMENTATION OF MICROSTRIP ANTENNA SYSTEM FOR RTLS 47
3.1 Design Methodology for the Microstrip Antenna System 48
3.2 Design and Implementation of the Microstrip Antenna Array with Butler Matrix 49
3.2.1 Design of the Rectangular Microstrip Patch Antenna 50
3.2.2 Design of the 4×4 Butler Matrix 52
3.2.2.1 Design of Quadrature Hybrid 54
3.2.2.2 Design of Crossover 57
3.2.2.3 Design of Phase Shifter 60
3.2.2.4 Design of Paths between a 4×4 Butler Matrix and a Planar Antenna Array 61
3.2.3 Analysis of Planar Microstrip Antenna Array with Butler Matrix 63
3.2.4 Radiation Pattern for Planar Microstrip Antenna Array 64
3.2.5 Simulation and Measured Results 66
3.3 Analysis, Design, and Implementation of an Aperture-Coupled Microstrip Antenna 77
3.3.1 Analysis of ACMSA Using Cavity Model 78
3.3.1.1 Resonant Frequency 78
3.3.1.2 Magnetic Field Component in x-direction 80
3.3.1.3 Magnetic Field Component in y-direction 82
3.3.1.4 Input Impedance 84
3.3.2 Circular Polarization Diversity with ACMSA 86
3.3.3 Geometry of ACMSA 87
3.3.4 Simulation and Measured Results 91
3.4 Conclusions 99

CHAPTER 4
NEW TECHNIQUE TO FIND THE ANGLE OF ARRIVAL 101
4.1 Proposed AOA Finding Technique 103
4.2 Design Methodology for the Proposed AOA Finding Technique 106
4.3 Results and Discussion 107
4.4 Hardware Implementation and Experimental Setup 109
4.5 Conclusions 116
CHAPTER 5
MODEL DEVELOPMENT AND IMPLEMENTATION FOR TIME OF ARRIVAL ESTIMATOR 117
5.1 Model Development of the TOA Estimator 118
5.1.1 Development of the Signal Subspace 118
5.1.2 Development of the Noise Subspace 122
5.1.3 Forward Correlation Matrix 123
5.1.4 New Technique to Estimate the Dimensions of the Signal Subspace 124
5.1.5 MUSIC Algorithm 126
5.2 Design Methodology for the TOA estimator 127
5.3 Simulation Results and Discussion 129
5.4 Hardware Implementation for TOA Estimator 133
5.4.1 Tag 134
5.4.2 Reader 135
5.5 Experimental Results and Discussion 140
5.6 Kalman Filter 146
5.7 Conclusions 150
CHAPTER 6
CONCLUSIONS AND FUTURE WORK 152
6.1 Conclusions 152
6.2 Future Work 153
6.2.1 Hardware Implementation of the Proposed RTLS 153
6.2.2 NLOS Mitigation 154
6.2.3 Multiple Access and Multiple User Interference. 154
6.2.4 Low Noise Amplifier (LNA) 155
PUBLICATIONS 156
REFERENCES 157
APPENDIX A 167
ADS Schematics to Design Path 3 and Path 4 of the Planar Microstrip Antenna Array with 4×4 Butler Matrix 167
APPENDIX B 170
RO4000® Series High Frequency Circuit Materials 170
APPENDIX C 171
Propagation Constant Inside the Cavity 171
APPENDIX D 172
Mode Coefficients in *x*-Direxion Inside the Cavity 172
APPENDIX E 173
Small Form Factor (SFF) Software Defined Radio (SDR) Development Platform 173

LIST OF TABLES

Table 2.1 Comparison between active RFID locating system and RTLS 22
Table 2.2 Estimating Q_n and R for Kalman filter 46
Table 3.1 Phases associated with the selected port of the 4×4 Butler matrix 53
Table 3.2 Comparison between the proposed antenna system for RTLS and the most common antennas 99
Table 4.1 Actual, simulated, and measured AOA 113
Table 5.1 Estimated accuracy and precision of the locating system 145
Table 5.2 Effect of R on the performance of the locating system 148
Table 5.3 Estimated accuracy and precision of the locating system before and after the use of Kalman filter 150

LIST OF FIGURES

Figure 1.1 Outline of the thesis 8
Figure 2.1 A-GPS operation (CommScope Inc, 2009) 11
Figure 2.2 Microstrip patch antenna for GPS application (Maxtena, 2009) 12
Figure 2.3 WLAN positioning based on fingerprinting technique (Kŭpper, 2005) 13
Figure 2.4 Omni-directional antennas for WLAN (a) Dipole antenna at 2.4 GHz (Linktek Technology, 2009). (b) Omni antenna at 2.4 GHz (Luxul Wireless, 2009) 14
Figure 2.5 Directional antennas for WLAN (a) PCB patch antenna at 2.4 GHz (Chinmore Industry Co, 2009). (b) Flat patch antenna at 2.4 GHz (Luxul Wireless, 2009) 14
Figure 2.6 Cooperative location estimation (Farahani, 2008) 15
Figure 2.7 Chip antennas for Zigbee (a) Small planar monopole antenna at 2.4 GHz (Fractus, 2009). (b) Zigbee module (MaxStream, 2009) 16
Figure 2.8 UWB Ubisense system (Ubisense, 2007) 17
Figure 2.9 Antennas for UWB positioning system (a) UWB Omni-directional antenna (2 dBi, 0.8 to 6 GHz) (European Antennas Ltd, 2009). (b) UWB bullet antenna (1.5 dBi, 2.4 to 6 GHz) (WIFI-PLUS Inc, 2008) 18
Figure 2.10 Directional antennas for UWB positioning system (a) UWB directional antenna (0.519 to 11.39 GHz) (TMR&D, 2009). (b) Planar spiral antenna (0.6 to 4 GHz, 3.4 dBi) (European Antennas Ltd, 2009) 19
Figure 2.11 Active RFID locating system 20
Figure 2.12 RTLS (a) Locate the tag based on distance information. (b) Locate the tag based on AOA information. (c) Locate the tag based on distance/AOA hybrid 22
Figure 2.13 Geometry of microstrip patch antenna 24
Figure 2.14 Microstrip line feed 25
Figure 2.15 Coaxial feed 25
Figure 2.16 Aperture coupled feed 26
Figure 2.17 Proximity coupled feed 26
Figure 2.18 Rectangular microstrip patch antenna 27
Figure 2.19 Analysis of microstrip antenna using ADS momentum 28
Figure 2.20 Layout of the Butler matrix and antenna array (Pham et al., 2005) 29
Figure 2.21 Two different arrangements for 2×2 microstrip array that generate circular polarization with linear polarization elements (Huang, 1986) 30
Figure 2.22 Measured radiation pattern for a dual circularly polarized antenna fed by L-strip (Wu et al., 2008) 30
Figure 2.23 Circularly polarized ACMSA excited by a symmetrical cross-slot (Al-Jibouri et al., 2001) 31
Figure 2.24 Reconfigurable microstrip patch antenna with a U-slot (Chung et al., 2006) 31
Figure 2.25 Reconfigurable microstrip patch antenna for switchable polarization (Sung et al., 2004) 32
Figure 2.26 Reconfigurable patch antenna using switchable slots (Fan et al., 2002) 32
Figure 2.27 Functional block diagram of TOA estimation using MUSIC algorithm (Xinrong et al., 2004) 34
Figure 2.28 Effect of multi-path on the spread spectrum locating system 35

Figure 2.29 Phase measurement for TOA estimation 36
Figure 2.30 Distance estimation using RSS 37
Figure 2.31 Spectral estimation using mechanical steering to find AOA 38
Figure 2.32 Spectral estimation using electronic steering to find AOA 38
Figure 2.33 AOA estimation using ML and eigen structure methods 40
Figure 2.34 Positioning based on the tri-lateration technique 41
Figure 2.35 Angle-Based technique to locate the tag 42
Figure 2.36 Positioning based on the TDOA technique 44
Figure 2.37 Locate the tag using distance/AOA hybrid 45
Figure 3.1 Design methodology for the microstrip antenna system 49
Figure 3.2 Inset fed rectangular microstrip patch antenna 50
Figure 3.3 Transmission line model of the rectangular microstrip patch antenna 51
Figure 3.4 Dependence of the input impedance on the distance into the patch 51
Figure 3.5 4×4 Butler matrix geometry 52
Figure 3.6 ADS schematic for 4×4 Butler matrix 53
Figure 3.7 ADS schematic for an ideal quadrature hybrid 54
Figure 3.8 ADS schematic for a real quadrature hybrid 55
Figure 3.9 Higher level ADS schematic to optimize the dimensions of the real quadrature hybrid 56
Figure 3.10 Simulated S-parameters of the real quadrature hybrid 57
Figure 3.11 ADS schematic for the ideal crossover 58
Figure 3.12 ADS schematic for the real microstrip crossover 58
Figure 3.13 Higher level ADS schematic to optimize the dimensions of the real crossover 59
Figure 3.14 Simulated S-parameters of the real crossover 60
Figure 3.15 Fabricated 4×4 Butler matrix 60
Figure 3.16 ADS schematic for the path connecting antenna 2 and Butler matrix 61
Figure 3.17 ADS schematic to modify the length of path 2 62
Figure 3.18 ADS simulated results for phases of path 2 and reference path 62
Figure 3.19 Phases associated with each port of the planar microstrip antenna array with 4×4 Butler matrix 64
Figure 3.20 Simulated normalized *E*-plane radiation pattern of the planar microstrip antenna array versus an elevation angle (— feed at port 1, –· feed at port 2, … feed at port 3, --- feed at port 4) 66
Figure 3.21 Simulated normalized *H*-plane radiation pattern of the planar microstrip antenna array versus an elevation angle (— feed at port 1, –· feed at port 2, … feed at port 3, --- feed at port 4) 67
Figure 3.22 Parameters setup in ADS Momentum for substrate layers of the Rogers's substrate 68
Figure 3.23 Parameters setup in ADS Momentum for metallization layers of the Rogers's substrate 69
Figure 3.24 ADS Momentum for the planar microstrip antenna array 69
Figure 3.25 ADS schematic diagram for simulating the planar microstrip antenna with 4×4 Butler matrix 70
Figure 3.26 ADS layout of the planar microstrip antenna array with 4×4 Butler matrix 71
Figure 3.27 Fabricated planar microstrip antenna array with 4×4 Butler matrix 71

Figure 3.28 Reflection coefficients versus frequency for the planar microstrip antenna array with 4×4 Butler matrix 72
Figure 3.29 Reflection coefficient versus frequency for an inset-fed rectangular microstrip patch antenna 73
Figure 3.30 Measured normalized radiation pattern of the planar microstrip antenna array with 4×4 Butler matrix at 2.437 GHz 74
Figure 3.31 Measured axial ratios of the planar microstrip antenna array with 4×4 Butler matrix at 2.437 GHz 75
Figure 3.32 Measuring a planar microstrip antenna with Butler matrix inside near field Satimo chamber 76
Figure 3.33 Simulated reflection coefficients versus frequency for the planar microstrip antenna array with 4×4 Butler matrix using FR4 substrate 77
Figure 3.34 Cavity model of the ACMSA 78
Figure 3.35 Position of the aperture paralleled to *x*-axis 81
Figure 3.36 Position of the aperture paralleled to *y*-axis 83
Figure 3.37 Circular polarization diversity with ACMSA 86
Figure 3.38 Geometry of the proposed ACMSA 87
Figure 3.39 Geometry of ACMSA with straight open microstrip stub line 88
Figure 3.40 ADS schematic model for straight open microstrip stub line 89
Figure 3.41 ADS schematic model for bended open microstrip stub line 89
Figure 3.42 ADS schematic to find the optimum length of the bended open microstrip stub line 90
Figure 3.43 Simulated responses for straight and bended open microstrip stub line 90
Figure 3.44 Simulated input impedance of the ACMSA without L_{os} 91
Figure 3.45 Simulated input impedance of the ACMSA with L_{os} 92
Figure 3.46 Reflection coefficient versus frequency when the right port of the quadrature hybrid is selected 92
Figure 3.47 Normalized measured radiation pattern when the right port of the quadrature hybrid is selected 93
Figure 3.48 Reflection coefficient versus frequency when the left port of the quadrature hybrid is selected 93
Figure 3.49 Normalized measured radiation pattern when the left port of the quadrature hybrid is selected 94
Figure 3.50 Parameters setup in ADS Momentum for substrate layers of the ACMSA 94
Figure 3.51 Parameters setup in ADS Momentum for metallization layers of ACMSA 95
Figure 3.52 Fabricated patch substrate 96
Figure 3.53 Fabricated feed substrate 96
Figure 3.54 Measured axial ratio at both ports of the ACMSA versus an elevation angle 97
Figure 3.55 Measuring aperture-coupled microstrip antenna inside Satimo chamber 97
Figure 4.1 AOA estimation techniques (a) Proposed AOA estimation technique. (b) AOA estimation using ML and eigen-structure methods 102
Figure 4.2 Proposed receiver block diagram to find AOA 103
Figure 4.3 Design Methodology for the proposed AOA estimation technique 106
Figure 4.4 Simulink model for simulating the proposed technique to find AOA 107
Figure 4.5 Generated AOA using the new technique (a) SNR= 1 dB, (b) SNR= 20 dB 109

Figure 4.6 Simulink model for hardware implementation of the proposed AOA estimator 109
Figure 4.7 Transmitter subsystem 110
Figure 4.8 Simulink subsystem for the AOA estimator 110
Figure 4.9 Signal is received by linear microphone array 111
Figure 4.10 Signal is received by single microphone 112
Figure 4.11 Speaker is located at different angles with respect to the microphone array 113
Figure 5.1 A received signal represented as summation of multiple paths of the transmitted signal 119
Figure 5.2 Processing of the received snapshot 124
Figure 5.3 Required computation time for the proposed technique, hypothesis testing approach, AIC technique and MDL technique versus the number of eigenvalues 126
Figure 5.4 Block diagram to find the MUSIC pseudo-spectrum 127
Figure 5.5 Design Methodology for the TOA estimator 128
Figure 5.6 Simulation model of the TOA estimator using simulink 129
Figure 5.7 Estimated TOA of each path versus MUSIC pseudo-spectrum 130
Figure 5.8 Effect of implementing zero-padding on the performance of the locating system 131
Figure 5.9 Effect of implementing FCM on the performance of the locating system 132
Figure 5.10 Received power versus the distance between tag and reader 133
Figure 5.11 Hardware implementation for TOA estimator 134
Figure 5.12 Simulink subsystem for the tag 134
Figure 5.13 IQ modulator 135
Figure 5.14 IQ demodulator 135
Figure 5.15 Simulink submodel for TOA estimator 137
Figure 5.16 Simulink subsystem to find FCM 138
Figure 5.17 Simulink subsystem to find IFFT for the noise subspace 140
Figure 5.18 Experimental setup for the TOA estimator 141
Figure 5.19 Position of the tag with respect to the reader 142
Figure 5.20 Simulink sub-model to find the error in the estimated TOA 143
Figure 5.21 Simulink sub-model to estimate the position of the tag 144
Figure 5.22 Finding the precision of the TOA estimator 145
Figure 5.23 Operation of the Kalman filter 149
Figure 5.24 Simulink sub-model to implement the Kalman filter with TOA estimator 149

LIST OF ABBREVIATIONS

ACMSA	Aperture-Coupled Microstrip Antenna
ADS	Advanced Design Software
A-GPS	Assisted- Global Positioning System
AOA	Angle-Of-Arrival
AWGN	Additive White Gaussian Noise
CCS	Code Composer Studio
CRLB	Cramer-Rao Lower Bound
DOA	Direction Of Arrival
DSSS	Direct Sequence Spread Spectrum
E-911	Enhanced 911 Service System
EVD	Eigen Value Decomposition
FCM	Forward Correlation Matrix
FFT	Fast Fourier Transform
GPS	Global Positioning System
IFFT	Inverse Fast Fourier Transform
ISI	Inter-Symbol Interference
LHCP	Left-Hand Circular Polarization
LNA	Low Noise Amplifier
LOS	Line Of Sight
MDL	Minimum Descriptive Length
MLM	Maximum Likelihood Method
MUSIC	MUltiple SIgnal Classification

NLOS	None Line Of Sight
OFDM	Orthogonal Frequency Division Multiplexing
PN	Pseudonoise
RFID	Radio Frequency Identification
RHCP	Right-Hand Circular Polarization
RSS	Received Signal Strength
RTLS	Real Time Locating Systems
SDR	Software-Defined Radio
SFF	Small FormFactor
SNR	Signal-to-Noise Ratio
STD	Standard Deviation
TDOA	Time Difference of Arrival
TLM	Transmission Line Model
TOA	Time-Of-Arrival
UWB	Ultra-Wideband
WLAN	Wireless Local Area Network
ZP	Zero Padding

LIST OF SYMBOLS

$\beta_{x,mn}$	Amplitude coefficient of (m, n) mode in x-direction inside the cavity
$\beta_{y,mn}$	Amplitude coefficient of (m, n) mode in y-direction inside the cavity
ε_o	Permittivity of free space
ε_r	Relative dielectric constant
θ	Elevation angle
θ_1	Angle of arrival between tag and reader 1
θ_2	Angle of arrival between tag and reader 2
θ_{AOA}	Angle of arrival
θ_{AOA_error}	Error in the angle of arrival
μ	Magnetic permeability
Σ	Diagonal eigenvalues matrix
Σ_{norm}	Normalized diagonal eigenvalues matrix
σ_n^2	Variance of the additive white Gaussian noise
σ_{noise}^2	Noise power of any received snapshot
σ_{signal}^2	Signal power of any received snapshot
σ_{TOA}^2	Minimum variance of the successive TOA samples
τ	Minimum time difference between two successive paths of the channel power delay profile
Φ	Phase difference between the received and the transmitted carrier signals

ϕ_x	Feeding phase for the antenna 4 of a planar microstrip antenna array
ϕ_y	Feeding phase for the antenna 2 of a planar microstrip antenna array
Ψ_{mn}	Eigen functions of the homogeneous wave equation
ω	Angular frequency
ω_c	Carrier frequency
A	Phase associated with antenna 1 of the planar microstrip antenna array
A_F	E-plane array factor for the planar microstrip array
$\left\|AF_{T_E}\right\|$	Normalized *E*-plane array factor for the planar microstrip array
$\left\|AF_{T_H}\right\|$	Normalized *H*-plane array factor for the planar microstrip array
A_{ss}	Signal subspace
A_{P1_Fg}	Generated array factor associated with port 1 of the Butler matrix
A_{P2_Fg}	Generated array factor associated with port 2 of the Butler matrix
A_{P3_Fg}	Generated array factor associated with port 3 of the Butler matrix
A_{P4_Fg}	Generated array factor associated with port 4 of the Butler matrix
A_{st}	State transition matrix for Kalman filter
a	Acceleration
B	Phase associated with antenna 2 of the planar microstrip antenna array
C	Phase associated with antenna 3 of the planar microstrip antenna **array**
C_F	Fringing effect in case of using TLM to design patch antenna
$CRLB_{TOA}$	Cramer Rao Lower Bound for the TOA estimator
c	Speed of light
c_s	Speed of sound

D	Phase associated with antenna 4 of the planar microstrip antenna array
d_x	Spacing distance between the patches in *x*-direction
d_y	Spacing distance between the patches in y-direction
dT	Elapsed time between the prediction and the correction steps
E	Electric field inside the cavity volume
E_{ay}	Electric field distribution in the aperture paralleled to *x*-axis
E_{ax}	Electric field distribution in the aperture paralleled to *y*-axis
E_x	Electric field in *x*-direction inside the cavity volume
E_y	Electric field in *y*-direction inside the cavity volume
E_z	Electric field in *z*-direction inside the cavity volume
E_θ	Total normalized *E*-plane radiation pattern of a single microstrip patch antenna
E_{x_planar}	Normalized instantaneous *E*-plane in *x*-direction for the planar microstrip antenna array
E_{y_planar}	Normalized instantaneous *E*-plane in *y*-direction for the planar microstrip antenna array
E_{T_θ}	Total normalized *E*-plane radiation pattern of a planar microstrip antenna array
$E(z,t)$	Instantaneous field of the plane wave traveling in positive *z*-direction
F	Fast Fourier Transform operation
F_n	Noise figure
f_{mn}	Resonance frequency of (*m*, *n*) mode inside the cavity

f	Frequency of the Nth subcarrier
G_{12}	Coupled conductance between the radiating slots of the patch antenna
$\overline{G}_k$	Predicted state at time k
$\widehat{G}_{k-1}$	Updated or the corrected state at time $k-1$
G_R	Radiation losses in case of using TLM to design the patch antenna
$Gain_{RX}$	Receive-side antenna gain in dBi
$Gain_{TX}$	Transmit-side antenna gain in dBi
H_θ	Total normalized *H*-plane radiation pattern of a single microstrip patch antenna
H	Magnetic field inside the cavity volume
H_m	measured matrix for Kalman filter
H_x	Magnetic field in *x*-direction inside the cavity volume
H_y	Magnetic field in *y*-direction inside the cavity volume
H_z	Magnetic field in *z*-direction inside the cavity volume
H_{T_θ}	Total normalized *H*-plane radiation pattern of a planar microstrip antenna array
h	Channel impulse response
h_t	Thickness of the Rogers's substrate
J_{mx}	Current density in the aperture parallel to *x*-axis
J_{my}	Current density in the aperture parallel to y-axis
K	Propagation constant inside the cavity
K_a	Wave number of the aperture
K_{eff}	Effective propagation constant

K_F	Wave number of the microstrip feed line
k_k	Kalman gain
K_m	Propagation constant of *m* mode
K_{mn}	Propagation constant of (*m*, *n*) mode
K_n	Propagation constant of *n* mode
K_o	Propagation constant in free space
L	Length of the microstrip patch antenna
L_a	Length of the aperture
L_{os}	Open microstrip stub line
$loss_{RX}$	Sum of all receive-side cable and connector losses in dB
$loss_{TX}$	Sum of all transmit-side cable and connector losses in dB
L_p	Number of multipaths of wireless channel
L_{zp}	Number of zeros added at the end of the transmitted signal
M_a	Number of the antenna array elements
M_{ax}	Magnetic current in the aperture parallel to *x*-axis
M_{ay}	Magnetic current in the aperture parallel to *y*-axis
M_s	Magnetic current in each radiating slot of the patch antenna
N	Number of subcarriers of the OFDM signal
N_{suc}	Number of successive TOA samples
n1	Transformation ratio which describes the coupling between the microstrip feed line and the patch
n_l	Path loss exponent.
n_{AF}	Total number of the generated array factors

n_a	AWGN
n_s	n_s th subcarrier of the received signal
$\overline{P}_k$	Predicted error covariance of the new state
$\hat{P}_{k-1}$	Updated or the corrected error covariance at time *k-1*
$\overline{P_k}$	Error covariance of the predicted state
$\hat{P_k}$	Updated error covariance at time *k*
PL_{1meter}	Reference path loss in dB when the receiver to transmitter distance is 1 meter
Q	Quality factor
Q_n	Process noise covariance for Kalman filter
R	measurement noise covariance matrix
R_{FCM}	Autocorrelation matrix of the received snapshots
$RL_{_in}$	Input return loss matrix
$RL_{_out}$	Output return loss
R_N	Device noise resistance
R_{YY}	Autocorrelation matrix of the received signal
RX_{PWR}	Detected received signal strength in dB
R_{array}	Received signal from any port of the Butler Matrix
R_{patch}	Received signal from a single patch antenna
r	Measured distance between the tag and the reader
r_1	Distances between reader 1 and tag
r_2	Distances between reader 2 and tag
r_3	Distances between reader 3 and tag

$r_{1,2}$	Measured difference range between r_1 and r_2
$r_{3,2}$	Measured difference range between r_3 and r_2
[S]	Scattering matrix
S	Transmitted signal in frequency domain
S_l	Degree of shadow fading
s	Width of the radiating slot of the patch antenna
T_{L_p}	Maximum delay spread of the wireless channel
$T_{L_{zp}}$	Zero padding time interval
T_s	Sampling time
T_{TOA}	Time of arrival
T_{TOA_error}	Error in the time of arrival
TX_{PWR}	Transmitter output power in dB
U	Output signal from the wireless channel
V	Volume occupied by the source within which the magnetic currents exist
V_{EVD}	Orthogonal eigenvectors matrix
V_S	Orthogonal eigenvectors related to signal
V_{noise}	Orthogonal eigenvectors related to noise
V_{ox}	Voltage at the middle of the aperture paralleled to the *x*-axis
V_{oy}	Voltage at the middle of the aperture paralleled to the *y*-axis
ν_{array}	Additive white Gaussian noise generated with a planar array
ν_{patch}	Additive white Gaussian noise generated with a single patch antenna
W	Width of the microstrip patch antenna

W_a	Width of the aperture
w_{k-1}	Process noise
X_1	Distance from the square patch edge to the center of the aperture
X_o	Distance into the inset fed patch antenna
x	Transmitted signal in time domain
(x_1, z_1)	Co-ordinates of reader 1
(x_2, z_2)	Co-ordinates of reader 2
(x_3, z_3)	Co-ordinates of reader 3
(X, Z)	Co-ordinates of the tag without error
(X', Z')	Co-ordinates of the tag with error
Y_1	Distance from the square patch edge to the center of the aperture
Y	Received signal in frequency domain
Y_{FCM}	Received snapshot after preprocessing before the autocorrelation
Y_{ap}	Admittance value of the aperture
$Y_{x,ant}$	Admittance of the patch in *x*-direction
$Y_{y,ant}$	Admittance of the patch in *y*-direction
y	Received signal in time domain
Z_{ca}	Characteristic impedance of the aperture
Z_F	Characteristic impedance of the microstrip feed line
Z_{in}	Input impedance of the ACMSA
Z_{in_stub}	Input impedance of the ACMSA with the open microstrip stub line

CHAPTER 1

INTRODUCTION

1.1 Motivation

There are increasing interests in the location-based applications in indoor environments. In RTLS, the determination of location information of the tag with respect to one or more reference reader creates a large number of applications. The commercial applications include asset and personal localization in warehouses and hospitals, locating elderly persons, locating children in public areas, guiding visitors in museums and many other similar scenarios. In public safety and military applications, they are used for navigating the firefighter, police men and soldiers to complete their missions inside or around the buildings. Also smart homes and offices that exploit the location information are few other examples of how our daily lives can be made easier with RTLS (Chia-Chin et al., 2006). The global RTLS market is expected to increase to 2710 million US dollars in 2016, while it was only 70 million US dollars in 2006 (Sahinoglu et al., 2008). The major applications of RTLS in 2016 are predicted to be in military (44%), health-care (30%), and other applications (26%) (Sahinoglu et al., 2008). Several locating technologies have been developed and commercialized which include the Global Positioning System (GPS) and the wireless enhanced 911 service system (E-911) which locates any phone that makes an emergency call. However, these locating technologies are used mainly for outdoor applications and could not be used effectively inside buildings and in dense urban areas (Djuknic et al., 2001). Moreover, the accuracy

requirements are dissimilar between indoor and outdoor environments. For an application such as E-911, an accuracy of 125 m 67% of the time is considered acceptable, while indoor applications require an accuracy level in the order of only a few meters. Wireless Local Area Network (WLAN) technology has recently become a candidate technology for indoor localization but its location accuracy is poor (Sahinoglu et al., 2008). Most of the commercial indoor localization systems provide a poor performance due to the presence of noise, interference, path loss, polarization mismatch, polarization reflection and the effect of the multi-path phenomenon in the indoor wireless channel (Saleh et al., 1987). Therefore, the need for a locating system which has good performance in indoor environments is quite obvious.

1.2 Problem Statement

The effect of path loss, interference, noise, polarization mismatch, polarization reflection, and multipath on the performance of a radio communications link continues to present one of the major challenges to wireless systems, especially for indoor dynamic environments. The polarization mismatch can degrade the signal by more than 20 dB in a linearly polarized system (Air-Stream Wireless, 2007). The effect of the reflection in a multipath channel can reflect Right-Hand Circular Polarization (RHCP) wave and change it to Left-Hand Circular Polarization (LHCP) wave or vice versa (Dinesh et al., 2006, Theodore, 2002). The received signal can be lost due to the effect of the polarization reflection if transmitting and receiving antennas do not have the same circular polarization sense (Air-Stream Wireless, 2007). The implementation of an antenna with a narrow beam-width helps to combat impairments such as path loss and

interference. The effects of the Polarization mismatch and the polarization reflection will be eliminated if both the transmitting and the receiving antennas have circular polarization diversity (Air-Stream Wireless, 2007). The implementation of circular polarization is more suitable for indoor wireless dynamic environments because it does not require an alignment between the transmitting and receiving antenna.

In this research, the topology of the RTLS consists of a mobile unit or a tag that can be considered as a signal transmitter, and one or more fixed measuring units or readers that receive the transmitter's signal. The transmitted signal from the tag is convolved with the channel impulse response due to which the time interval of the transmitted signal would be stretched and the Inter-Symbol Interference (ISI) might occur. The effect of ISI could degrade the performance of TOA estimator, but this effect could be mitigated by the insertion of zero-padding at the end of the transmitted signal. Practically the orthogonality between the subcarriers of the OFDM signal is destroyed due to the effect of fading in an indoor wireless channel. The orthogonality between these subcarriers is retrieved by using the Forward Correlation Matrix (FCM) technique. In this technique the received signal is pre-processed before finding the autocorrelation matrix (Xinrong et al., 2004, Tie-Jun et al., 1985).

Most of the RTLS in the market require two or more readers to determine the coordinates of tag (Ubisense, 2007), Also the RTLS which are based on the Wi-Fi standard requires at least three access points to locate the tag (Ekahau, 2007, AeroScout, 2007). The RTLS from RF Code company which has room level accuracy requires one reader in addition to room locator at each room in the building (RF Code, 2008). The estimation of the AOA provides the ability to determine the position of the tag using only one reader based on the joint (TOA/AOA) information or the joint (Received

Signal Strength (RSS)/AOA) information. Although, the estimation of the AOA provides the ability to use only one reader and to minimize the infrastructure of the locating system, the conventional AOA estimation techniques require high hardware complexity. In this research, a new technique is used to estimate the AOA without spatial sampling, so that the hardware requirement is less compared to the other conventional methods.

1.3 Objectives

The objective of the research work as described in this thesis is to realize the real time locating systems that can achieve the following requirements:

- To combat the major impairments of indoor wireless dynamic environments.
- To improve the performance of the locating system in indoor wireless dynamic environments.
- Possibility to minimize infrastructure and reduce hardware complexity of the locating system.

1.3.1 To Combat the Major Impairments of Indoor Wireless Dynamic Environments

The major challenges to indoor wireless dynamic environments are combated by developing 2.4 GHz antenna system to be implemented with RTLS. At the reader, four beams that have circular polarization diversity, high gain, good axial ratio and wide bandwidth are obtained by implementing the 4×4 Butler matrix as a feeding network to the 2×2 microstrip antenna array. The Aperture-Coupled Microstrip Antenna (ACMSA)

can be utilized with the tag or the reader because it has circular polarization diversity, wide bandwidth, good axial ratio and small size.

1.3.2 To Improve the Performance of the Locating System in Indoor Wireless Dynamic Environments

In a locating system, the most important performance metrics are the ranging accuracy and precision. The accuracy is defined as an error distance between the estimated location and the true location, while the precision is reported as the percentage of time to perform an acceptable location detection (Sahinoglu et al., 2008, Kamol, 2005). The accuracy and the precision of the locating system are improved by estimating the TOA based on MUltiple SIgnal Classification (MUSIC) algorithm, and implementing zero-padding and FCM with the TOA estimator. Also, the implementation of the Kalman filter improves the accuracy and the precision of the locating system.

1.3.3 Possibility to Minimize Infrastructure and Reduce Hardware Complexity of the Locating System

The minimal infrastructure of the locating system can be achieved by implementing the joint information of the (TOA/AOA) or the joint information of the (RSS/AOA) to determine the position of the tag using only one reader. Also, the hardware complexity is reduced by proposing a new technique to estimate the AOA without spatial sampling.

1.4 Contributions of the Thesis

The original work presented in this thesis is innovative in the following aspects:

- In the previous works, only one circularly polarized beam without diversity was generated by implementing a feeding network that produced four orthogonal phases (i.e. 0°, 90°, 180°, and 270°). In the present study, the planar antenna array has four beams in four different directions, circular polarization diversity, good axial ratio, high gain, and wide bandwidth. These advantages are gained from the four generated orthogonal phases at each input of the 4×4 Butler matrix which is implemented as a feeding network to the planar antenna array.
- The Aperture-Coupled Microstrip Antenna (ACMSA) is analyzed based on the cavity model theory to calculate the input impedance of the ACMSA. As far as we are aware, the ACMSA which has a square patch and fed by a quadrature hybrid has not been analyzed previously.
- In this research a new technique is developed to find the AOA based on processing of two received signals; one of them is received by an antenna array and the other is received from a single element which is identical to the array elements.
- Development, simulation, and hardware implementation for the TOA estimator to investigate the effects of the variation of SNR and the implementation of zero-padding and Forward Correlation Matrix (FCM) on the system performance.
- New techniques are developed to estimate the number of paths of the received signal and to find the MUSIC pseudo-spectrum.

- The CRLB is a theoretical lower bound which is used to predict the smallest error that can be achieved (Xu et al., 2008). In this research, the CRLB is implemented in real time as a part of the TOA estimator to determine the error in measured TOA value.
- Developed a new method to find the value of the measurement noise covariance matrix to improve the performance of the Kalman filter in wireless indoor dynamic environments.

1.5 Outline of the thesis.

This thesis is focused on the development of an antenna system and signal processing techniques to build an efficient and economical RTLS. Following the introduction (Chapter 1), a survey to introduce the wireless-based indoor positioning systems is done and then the literature review is discussed on the design and implementation of antennas for indoor wireless systems and the signal processing techniques for RTLS (Chapter 2). The remaining part of the thesis is organized as shown in Figure 1.1. Chapter 3 is divided into two main parts. The first part deals with the design methodology for microstrip antenna system, the design of rectangular patch antenna, the design of a 4×4 Butler matrix, the mathematical representation of a planar microstrip antenna array with Butler matrix, the development of the radiation pattern for planar microstrip antenna array and discussion on the simulated and measured results. In the second part, the analysis of ACMSA using cavity model is introduced and the circular polarization diversity with ACMSA is presented followed by the discussion on simulated and measured results. Chapter 4 presents the proposed technique to find AOA and the development of its mathematical representation, along with the results and discussion.

Hardware implementation and experimental setup are also introduced at the end of this chapter.

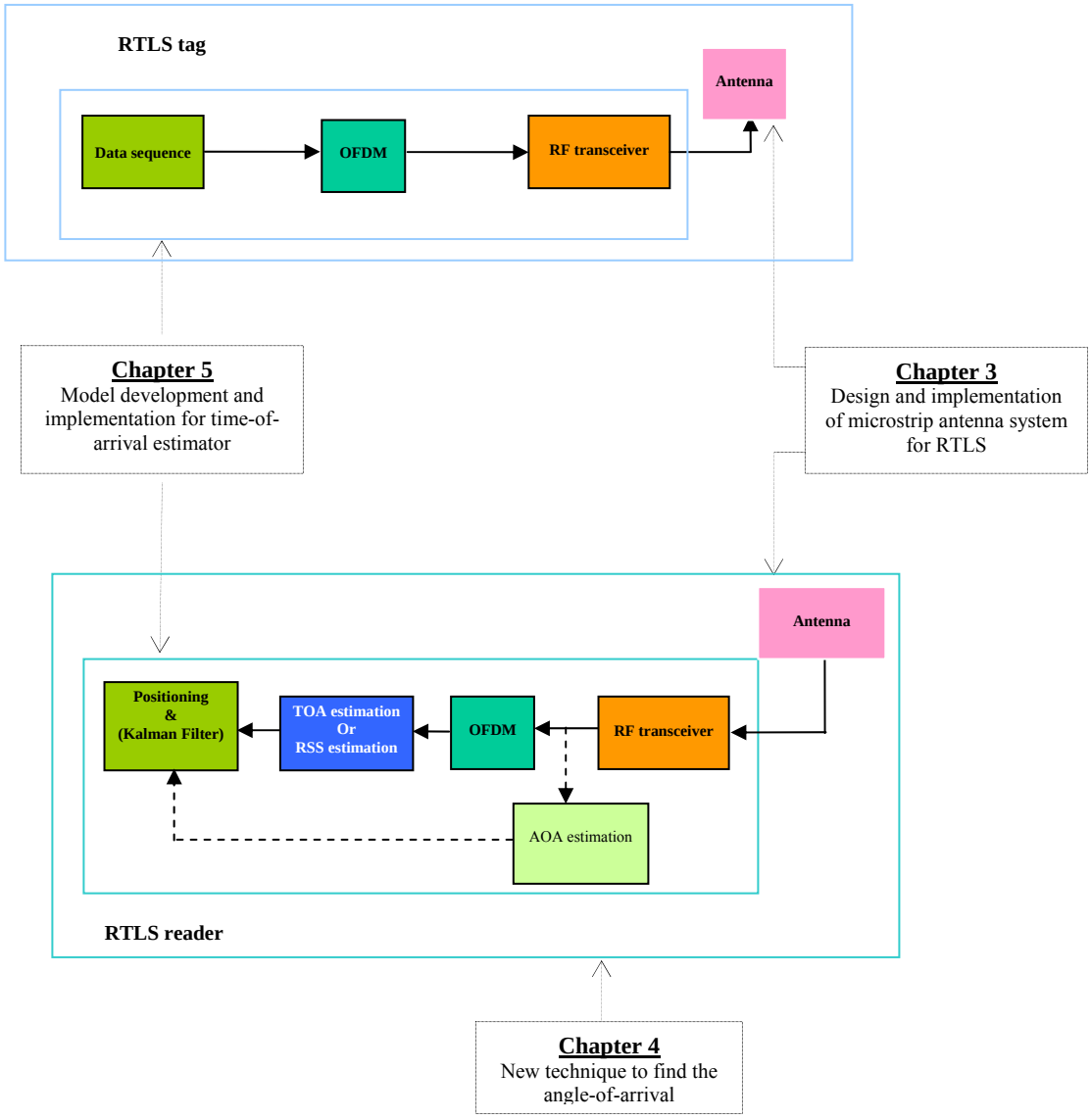

Figure 1.1 Outline of the thesis

In chapter 5, the development of the signal subspace and the noise subspace for the proposed TOA estimator is described. Further, FCM is discussed, a new technique to

estimate the dimensions of the signal subspace is introduced, the MUSIC algorithm is presented. Finally the simulation results are discussed and the real time hardware implementation for the TOA estimator is presented. The major conclusions and suggested future work are provided in chapter 6.

CHAPTER 2

LITERATURE REVIEW

This chapter provides an exhaustive review of the previous works pertaining to the current research. The survey of the wireless-based indoor positioning systems is presented in Section 2.1. The literature background of design and implementation of antennas for indoor wireless systems is presented in Section 2.2. Finally the literature review of the signal processing techniques for RTLS is provided in Section 2.3.

2.1 Survey of the Wireless-Based Indoor Positioning Systems

Several types of wireless technologies are used for indoor localization. The main wireless indoor positioning systems currently in practice are GPS, WLAN, ZigBee, Ultra-Wide Band (UWB), active Radio Frequency Identification (RFID) and RTLS.

2.1.1 GPS

GPS is a typical example of an outdoor localization system. It was developed in the early 1970s for military applications and is the most popular commercial location system today. It uses Time Difference Of Arrival (TDOA) information from four or more of 24 satellites around the world to estimate the position. Though GPS has fine precision outdoors, it fails to provide the desired accuracies in indoor environments due to the multipath effects and blocked LOS. In addition, GPS devices are usually expensive (Caffery, 2000, Sahinoglu et al., 2008). Assisted-GPS (A-GPS) has been developed to overcome the limitations of the conventional GPS, the accuracy of A-GPS has an

average of 5-50 m in indoor environments (Hui et al., 2007). A-GPS is a handset-based mobile which receives GPS signals from multiple GPS satellites and GPS assistance information from wireless mobile network as shown in Figure 2.1. If the handset-based mobile receives a weak signal from the GPS satellites, it will use the GPS assistance information from wireless mobile network to improve the localization performance.

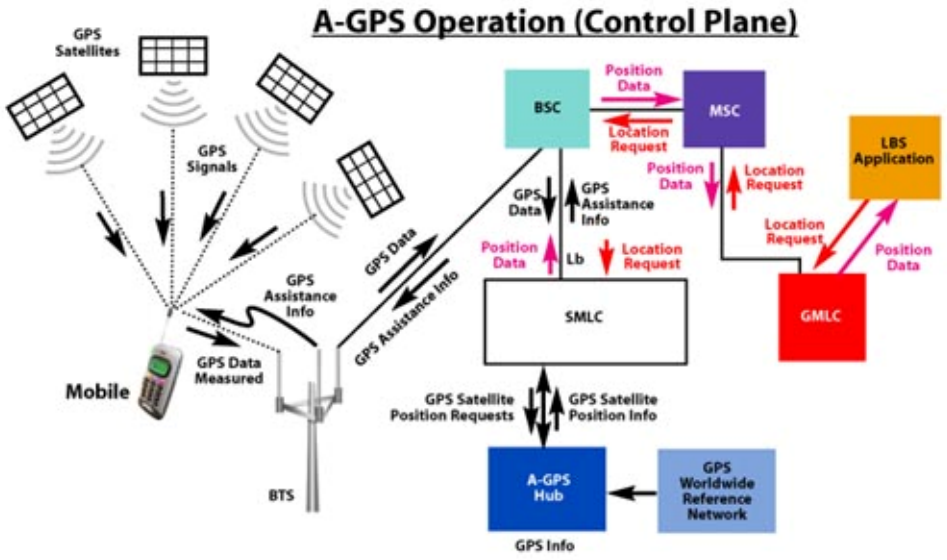

Figure 2.1 A-GPS operation (CommScope Inc, 2009)

The microstrip patch antenna is one of the most popular GPS antennas. The RHCP is crucial to GPS antenna (Dinesh et al., 2006). Figure 2.2 shows the microstrip patch antenna which has RHCP and its gain is 4.8 dBi, this antenna is suitable for GPS application (Maxtena, 2009).

Figure 2.2 Microstrip patch antenna for GPS application (Maxtena, 2009)

2.1.2 WLAN

Almost all WLAN locating systems are based on the measurements of the RSS and have accuracy between 3 to 30 m (Hui et al., 2007). Although WLAN has low accuracy, it avoids expensive deployment of infrastructure. Precise timing synchronization is a very difficult issue in WLAN, hence timing measurements are not possible. In WLAN, there are three basic positioning methods (Küpper, 2005):

- **Proximity sensing**. The position of the terminal is obtained by scanning all access points and finding the position of the access point that sends the strongest signal to the terminal.
- **Lateration.** The position of the terminal is obtained by determining the distance between the terminal and the access point based on the received RSS.
- **Fingerprinting**. This technique requires a training phase (off-line phase) to collect location fingerprints for all positions in the operating area before the actual deployment (on-line phase). In off-line phase, the site of interest is covered by a grid. The observer collects a vector of RSS values or a fingerprint from multiple access points at each point of the grid. In on-line phase, the terminal receives a vector of RSS values from multiple access points and reports

this RSS vector to a server. The server then tries to match the RSS vector with the fingerprints generated in the off-line phase to estimate the position of the terminal. The matching can also be performed locally as shown in Figure 2.2.

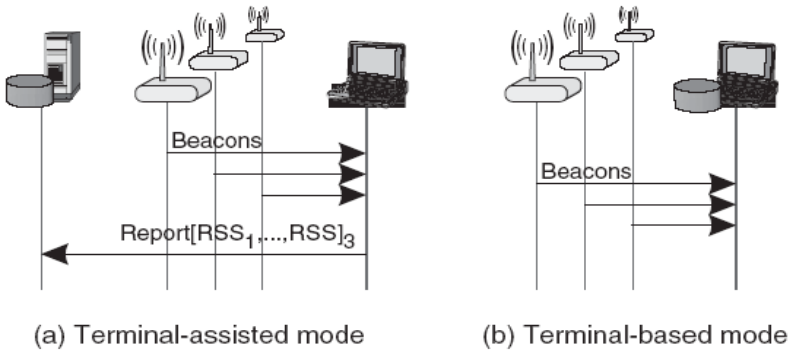

Figure 2.3 WLAN positioning based on fingerprinting technique (Küpper, 2005)

There are two basic types of antennas for WLAN: omni-directional and directional. The omni-directional antennas for WLAN can be linearly or circularly polarized. Figure 2.4 (a) shows a linearly polarized omni-directional antenna which has gain equal to 1.8 dBi (Linktek Technology, 2009), while circularly polarized omni-directional antenna with gain equal to 5 dBi is shown in Figure 2.4 (b) (Luxul Wireless, 2009).

(a)

(b)

Figure 2.4 Omni-directional antennas for WLAN (a) Dipole antenna at 2.4 GHz (Linktek Technology, 2009). (b) Omni antenna at 2.4 GHz (Luxul Wireless, 2009)

The directional antennas for WLAN provide a circular and linear polarization. Figure 2.5 (a) shows a directional and linearly polarized antenna which has gain equal to 8 dBi (Chinmore Industry Co, 2009), while 7 dBi circularly polarized directional antenna is shown in Figure 2.5 (b) (Luxul Wireless, 2009).

(a)

(b)

Figure 2.5 Directional antennas for WLAN (a) PCB patch antenna at 2.4 GHz (Chinmore Industry Co, 2009). (b) Flat patch antenna at 2.4 GHz (Luxul Wireless, 2009)

2.1.3 ZigBee

ZigBee locating system uses IEEE 802.15.4 standard. It is simple, low-cost and has accuracy of several meters (Farahani, 2008). ZigBee has a range of 10 to 100 meters with data capacities of 250 KB/s at 2.4 GHz, 40 KB/s at 915 MHz and 20 KB/s at 868 MHz. The localization in ZigBee is based on RSS, TOA and AOA location estimation methods. Among these three methods, the RSS method is the most dominant owing to its minimum hardware requirement. RSS can be implemented using proximity sensing, lateration, fingerprinting and cooperative location estimation. In cooperative location estimation, the ZigBee node that is being tracked broadcasts a signal to at least three ZigBee nodes with known fixed positions and the relative distances to each other of the tracked nodes are measured. The distances from the tracked node to the fixed nodes and the distances between the tracked nodes are processed to calculate the location of the tracked node as shown in Figure 2.3. The cooperative method helps to refine the location estimation accuracy beyond the achievable accuracy in a basic trilateration method but it can become computationally intensive (Farahani, 2008).

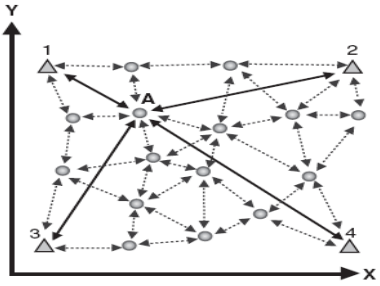

A fixed node with known location (anchor nodes).
A tracked node.
Estimated distance between a tracked node and an anchor node.
Estimated distance between two tracked nodes.

Figure 2.6 Cooperative location estimation (Farahani, 2008)

The chip antennas are commonly used for Zigbee. While the chip antennas provide the smallest antenna, the size reduction comes at a cost both in performance and pricing. The omni-directional linearly polarized chip antenna which has gain equal to 2 dBi at 2.4 GHz is shown in Figure 2.7 (a) (Fractus, 2009), this chip antenna can be integrated with the Zigbee as shown in Figure 2.7 (b) (MaxStream, 2009).

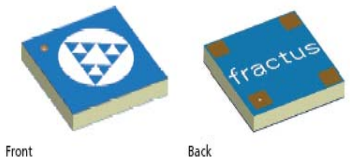

(a)

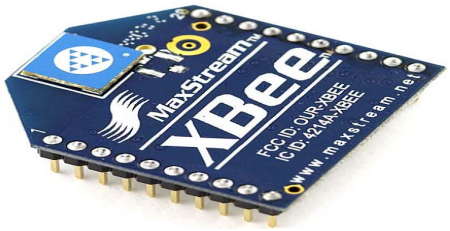

(b)

Figure 2.7 Chip antennas for Zigbee (a) Small planar monopole antenna at 2.4 GHz (Fractus, 2009). (b) Zigbee module (MaxStream, 2009)

In some indoor positioning applications, the size of the Zigbee nodes is not require to be small, so that several other antenna types that have a high gain and/or a circular polarization can be used to improve the performance of the Zigbee locating system (MaxStream, 2009).

2.1.4 UWB

UWB systems operate using radio signals having very wide bandwidth. The position of the tag can be determined based on TOA techniques (Sahinoglu et al., 2008). RSS technique is not implemented with this system. Although UWB can achieve very high indoor localization accuracy (20 cm) (Hui et al., 2007), this system is more sensitive to timing synchronization, requires high sampling rate and its coverage area is short. Moreover UWB hardware is expensive to purchase and scale. Figure 2.4 shows the Ubisense system which is UWB real-time locating system. The accuracy of this system is 30 cm and its maximum coverage area does not exceed 50 m (Hui et al., 2007).

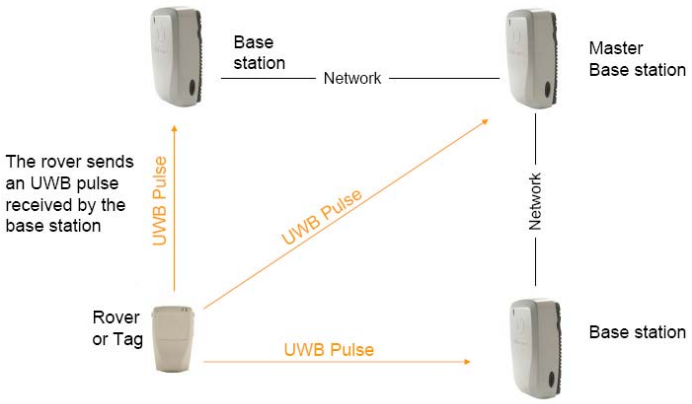

Figure 2.8 UWB Ubisense system (Ubisense, 2007)

The antennas for UWB positioning system are divided into omni-directional and directional. The UWB omni-directional antennas can be linearly polarized as shown in Figure 2.9 (a) or circularly polarized as shown in Figure 2.9 (b) (European Antennas Ltd, 2009, WIFI-PLUS Inc, 2008).

(a)

(b)

Figure 2.9 Antennas for UWB positioning system (a) UWB Omni-directional antenna (2 dBi, 0.8 to 6 GHz) (European Antennas Ltd, 2009). (b) UWB bullet antenna (1.5 dBi, 2.4 to 6 GHz) (WIFI-PLUS Inc, 2008)

The UWB directional antennas can provide a linear or circular polarization. Figure 2.10 (a) shows a linearly polarized UWB directional antenna, this antenna is matched over a bandwidth from 0.519 to 11.39 GHz (TMR&D, 2009). Figure 2.10 (b) shows UWB directional antenna which has circular polarization diversity and matched over a bandwidth from 0.6 to 4 GHz (European Antennas Ltd, 2009).

(a)

(b)

Figure 2.10 Directional antennas for UWB positioning system (a) UWB directional antenna (0.519 to 11.39 GHz) (TMR&D, 2009). (b) Planar spiral antenna (0.6 to 4 GHz, 3.4 dBi) (European Antennas Ltd, 2009)

2.1.5 Active RFID

The active RFID can be used as an indoor locating system. The active RFID locating system consists of tags and readers which are connected to a master station or PC through Ethernet or serial cables (RF Code, 2008). Each reader is fixed at a different room of the building and receives a signal from the tag, then the PC collects all signals from these readers and determines which one of these readers has strongest signal. The tag is located at the same room which includes the reader that sends the strongest signal (Muhammad, 2007). As shown in Figure 2.11, if the tag is closest to reader 2 which is fixed at room 2, so that the received signal by reader 2 is the strongest signal and the tag is located at room 2. The active RFID locating system determines the room at which the tag is located, but it can not find the exact location of the tag inside this room.

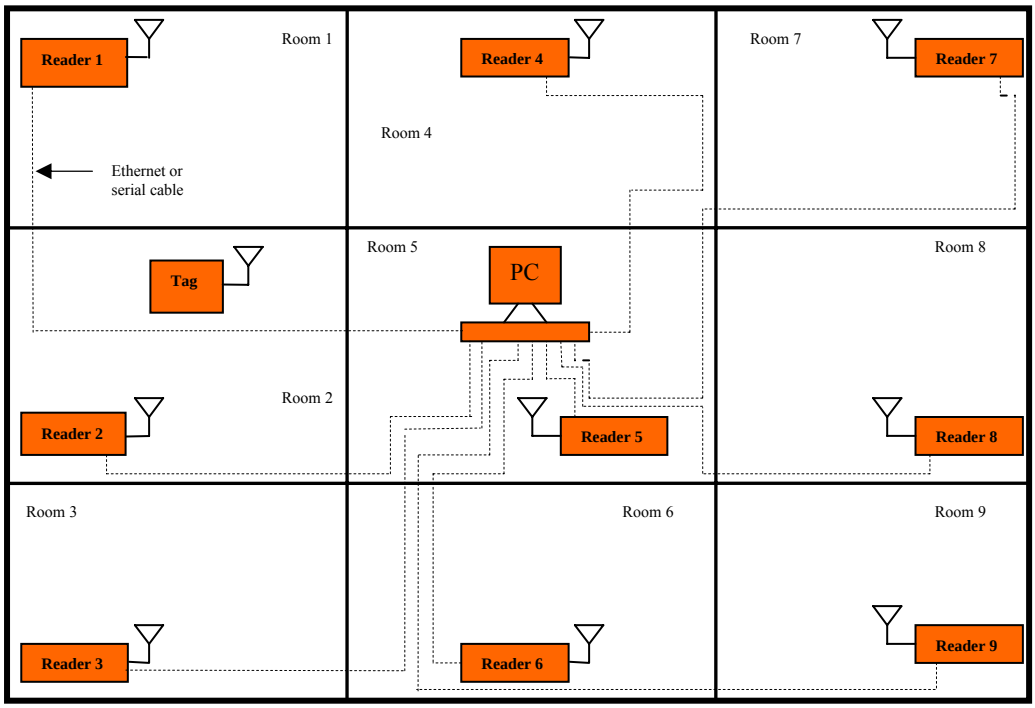

Figure 2.11 Active RFID locating system

The antenna types for WLAN can be used with 2.4 GHz active RFID (Chinmore Industry Co, 2009, Luxul Wireless, 2009, Linktek Technology, 2009), also the chip antennas can be implemented with the active RFID tags in the applications that require the size of the tag to be very small (Fractus, 2009).

2.1.6 RTLS

RTLS are able to provide the location of the people and assets when required. The RTLS consists of tags, readers, and a master station or a PC. In RTLS, the location of the tag is determined based on measuring the distance and/or the AOA between this tag and readers (Hui et al., 2007, Pahlavan et al., 2002). At least three readers are required to find the coordinates of the tag by using the measured distances between the tag and each

one of these readers as shown in Figure 2.12 (a). Two readers are required to locate the tag by using the AOA information as shown in Figure 2.12 (b). The position of the tag can be determined by using only one reader based on measuring both of the distance and the AOA between the tag and the reader as shown in Figure 2.12 (c).

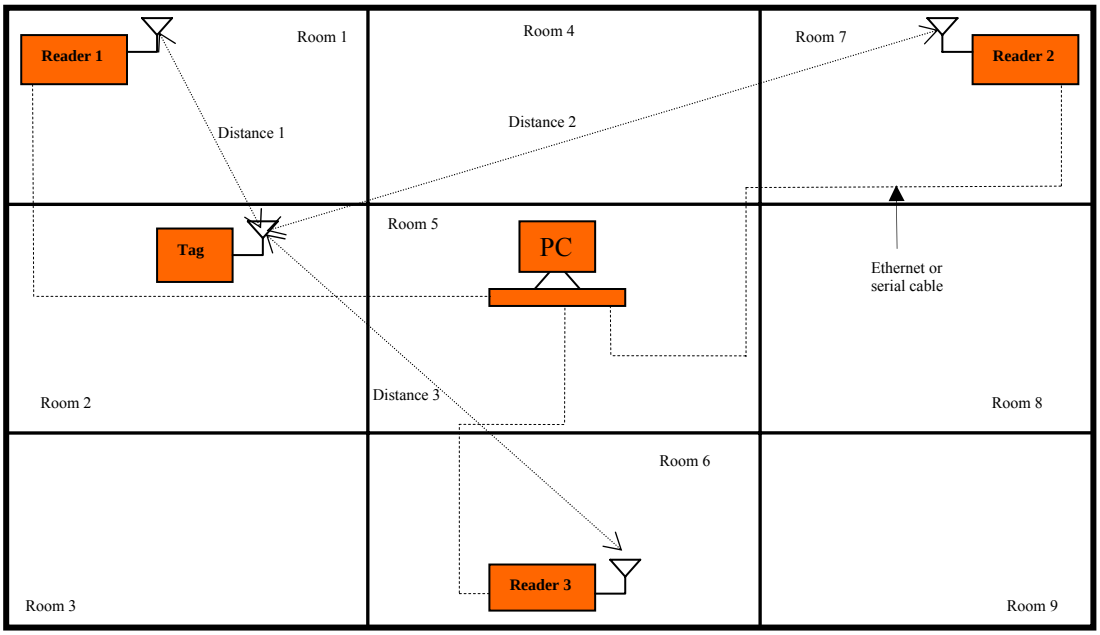

(a)

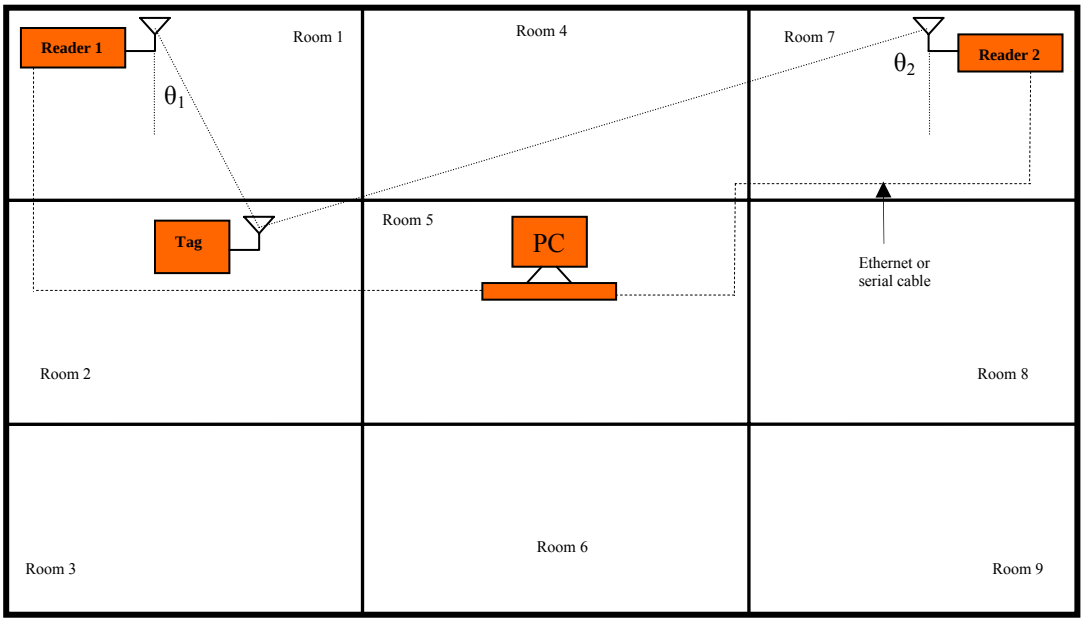

(b)

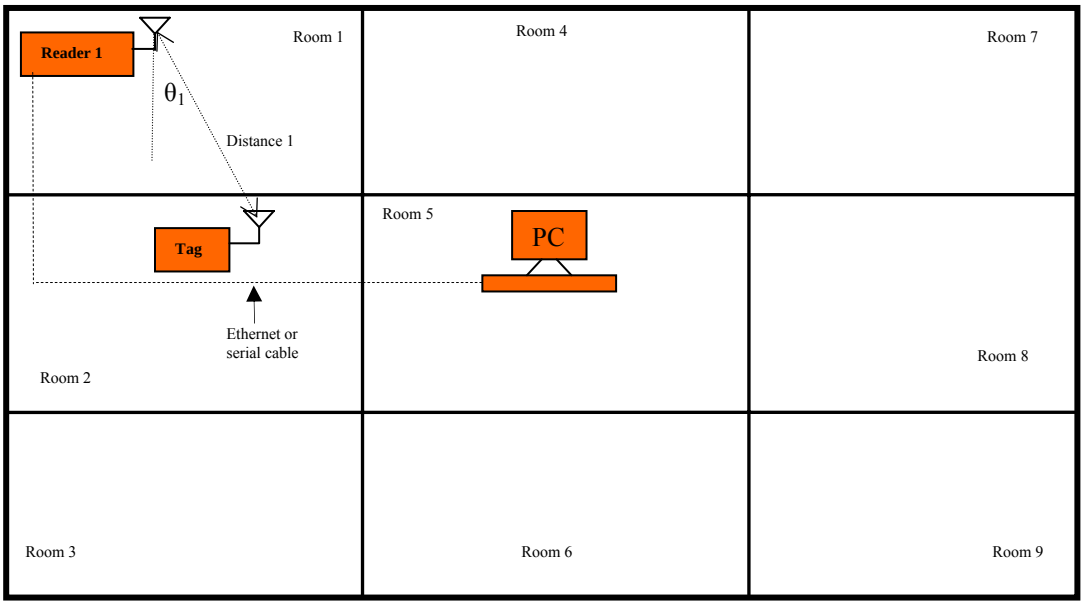

(c)

Figure 2.12 RTLS (a) Locate the tag based on distance information. (b) Locate the tag based on AOA information. (c) Locate the tag based on distance/AOA hybrid

There are many differences between the active RFID locating system and the RTLS, these differences are summarized in Table 2.1.

Table 2.1 Comparison between active RFID locating system and RTLS

	RTLS	Active RFID locating system
Location parameters	▪ Estimation of the distance between the tag and the reader based on the value of the TOA or the value of RSS. ▪ Estimation of the AOA of the signal which. is transmitted from the tag to the reader.	Scanning all readers and finding the position of the reader that sends the strongest signal to the master station.
Positioning methods	▪ Distance-based (tri-lateration). ▪ Angle-based (tri-angulation). ▪ Hyperbolic positioning technique. ▪ Positioning based on the distance/AOA hybrid.	Positioning methods are not implemented with the active RFID locating system.
Infrastructure	RTLS requires three readers, two readers, or one reader based on the positioning method.	One reader is required at each room of the building.
Accuracy	RTLS can achieve accuracy less than 1 m.	Room level accuracy

The antenna types for the active RFID locating system can be implemented with the RTLS (Chinmore Industry Co, 2009, Luxul Wireless, 2009, Fractus, 2009, Linktek Technology, 2009).

2.2 Design and Implementation of Antennas for Indoor Wireless Systems

This section provides a literature background of the most common methods employed to build up microstrip antenna, and a literature review of the previous works pertaining to the design and implementation of antennas which can be used with indoor wireless systems.

2.2.1 Most Common Methods Employed to Build up Microstrip Antenna

As the frequency used for a radio communication system gets higher, the size of the antenna gets smaller. Microstrip antennas are widely used in the frequency range above 1 GHz because the size of microstrip antennas at this frequency range is usually small. The microstrip antenna consists of a patch of metal on the top of a grounded dielectric substrate as shown in Figure 2.13. The microstrip antenna has been implemented due to its small size, low profile and cheap manufacturing costs. This section starts by presenting the feeding techniques for the microstrip antennas, followed by the methods for the analysis of microstrip antennas.

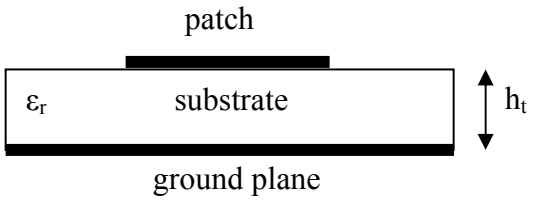

Figure 2.13 Geometry of microstrip patch antenna

2.2.1.1 Feeding Techniques

Feeding technique is an important design parameter because it influences the characteristics of the antenna. There are a variety of methods to feed the microstrip patch antennas. The feeding is done directly by a microstrip line or by a coaxial probe. It can also be done indirectly using an aperture coupling or using a proximity coupling (Kumar et al., 2003).

2.2.1.1.1 Microstrip Line Feed

This feed technique can be etched on the same substrate to provide a planar structure. Although the fabrication of the microstrip antennas based on this technique is simple, the feed radiation leads to undesired cross polarized radiation. The matching between the feed line to the patch can be done by using an additional matching element or an inset cut in the patch as shown in Figures 2.14 (a), and 2.14 (b), respectively (Kumar et al., 2003). Also the feed line can be matched with the patch using non radiating edge feed as shown in Figure 2.14 (c) (Ismail, 2003).